


RESEARCH ARTICLE | *Vascular Biology and Microcirculation*

## Sex differences in the structure and function of rat middle cerebral arteries

Shaoxun Wang,<sup>1</sup> Huawei Zhang,<sup>1</sup> Yedan Liu,<sup>1</sup> Longyang Li,<sup>1</sup> Ya Guo,<sup>1</sup> Feng Jiao,<sup>1,2</sup> Xing Fang,<sup>1</sup> Joshua R. Jefferson,<sup>1</sup> Man Li,<sup>1</sup> Wenjun Gao,<sup>1</sup> Ezekiel Gonzalez-Fernandez,<sup>1</sup> Rodrigo O. Maranon,<sup>3</sup>  Mallikarjuna R. Pabbidi,<sup>1</sup> Ruen Liu,<sup>2</sup> Barbara T. Alexander,<sup>4</sup> Richard J. Roman,<sup>1</sup> and Fan Fan<sup>1</sup>

<sup>1</sup>Department of Pharmacology and Toxicology, University of Mississippi Medical Center, Jackson, Mississippi; <sup>2</sup>Department of Neurosurgery, Peking University People's Hospital, Beijing, China; <sup>3</sup>Department of Cell and Molecular Biology, University of Mississippi Medical Center, Jackson, Mississippi; and <sup>4</sup>Department of Physiology and Biophysics, University of Mississippi Medical Center, Jackson, Mississippi

Submitted 9 December 2019; accepted in final form 23 March 2020

**Wang S, Zhang H, Liu Y, Li L, Guo Y, Jiao F, Fang X, Jefferson JR, Li M, Gao W, Gonzalez-Fernandez E, Maranon RO, Pabbidi MR, Liu R, Alexander BT, Roman RJ, Fan F.** Sex differences in the structure and function of rat middle cerebral arteries. *Am J Physiol Heart Circ Physiol* 318: H1219–H1232, 2020. First published March 27, 2020; doi:10.1152/ajpheart.00722.2019.—Epidemiological studies demonstrate that there are sex differences in the incidence, prevalence, and outcomes of cerebrovascular disease (CVD). The present study compared the structure and composition of the middle cerebral artery (MCA), neurovascular coupling, and cerebrovascular function and cognition in young Sprague-Dawley (SD) rats. Wall thickness and the inner diameter of the MCA were smaller in females than males. Female MCA exhibited less vascular smooth muscle cells (VSMCs), diminished contractile capability, and more collagen in the media, and a thicker internal elastic lamina with fewer fenestrae compared with males. Female MCA had elevated myogenic tone, lower distensibility, and higher wall stress. The stress/strain curves shifted to the left in female vessels compared with males. The MCA of females failed to constrict compared with a decrease of  $15.5 \pm 1.9\%$  in males when perfusion pressure was increased from 40 to 180 mmHg. Cerebral blood flow (CBF) rose by  $57.4 \pm 4.4$  and  $30.1 \pm 3.1\%$  in females and males, respectively, when perfusion pressure increased from 100 to 180 mmHg. The removal of endothelia did not alter the myogenic response in both sexes. Functional hyperemia responses to whisker-barrel stimulation and cognition examined with an eight-arm water maze were similar in both sexes. These results demonstrate that there are intrinsic structural differences in the MCA between sexes, which are associated with diminished myogenic response and CBF autoregulation in females. The structural differences do not alter neurovascular coupling and cognition at a young age; however, they might play a role in the development of CVD after menopause.

**NEW & NOTEWORTHY** Using perfusion fixation of the middle cerebral artery (MCA) in calcium-free solution at physiological pressure and systematically randomly sampling the sections prepared from the same M2 segments of MCA, we found that there are structural differences that are associated with altered cerebral blood flow (CBF) autoregulation but not neurovascular coupling and cognition in young, healthy Sprague-Dawley (SD) rats. Understanding the intrinsic differences in cerebrovascular structure and function in males and females is essential to develop new pharmaceutical treatments for cerebrovascular disease (CVD).

cerebral blood flow autoregulation; cognitive function; distensibility; myogenic response; sex difference

### INTRODUCTION

Epidemiological studies have clearly indicated that there are sex differences in the incidence, prevalence, and outcomes of cerebrovascular disease (CVD), including stroke and dementia. Young women are protected from CVD through adulthood but are at higher risk after the onset of menopause than men (30, 62, 66). Hormone replacement therapy does not reduce CVD risk in postmenopausal women in clinical trials (69, 79), suggesting that changes in the levels in sex hormones are not the sole contributing factor to the sex differences in cerebral vascular disease. Therefore, a better understanding of the intrinsic differences in the cerebral vasculature in male and female subjects and the influence of this divergence to vascular function will provide essential insight into CVD biology for the development of new pharmaceutical targets to improve treatments of CVD.

The most common pathologically affected aspect of the cerebral vasculature is the middle cerebral artery (MCA). As the largest branch of the internal carotid artery, the MCA provides blood supply to the lateral convexity of the hemisphere, including frontal, parietal, temporal, and occipital lobes, as well as the lateral sulcus, insula cortex, lenticular nucleus, and internal capsule (52, 85). Ischemic stroke comprises 85%, and 15% is hemorrhagic stroke (67). Embolism of the lenticulostriate branches of the MCA is the most common cause of ischemic stroke; ~33% of saccular aneurysms (the most common subtype of aneurysm) are found in the MCA, and aneurysm disruption is the most common cause of hemorrhagic stroke (52). Stroke survivors face long-term disability and cognitive deficits (37). Previous studies demonstrated that females have smaller MCA compared with males in humans (45, 51, 64) and in rats (61). The MCA in females has greater responses to hypercapnia, nitric oxide (NO), and flow-mediated vasodilation (31, 47, 54, 56) and lower responses to angiotensin II (ANG II) as well as endothelin-1 (ET-1)-induced vasoconstriction (1, 62).

The smaller MCA in females is associated with the elevated basal vascular tone and enhanced flow velocity under hypercapnia conditions (47, 54). Females have lower artery compliance (70, 77). Moreover, females have higher cerebral blood

Correspondence: F. Fan (e-mail: ffan@umc.edu).

flow at rest and during cognitive activities (35, 56), although the underlying mechanisms are not well understood.

The present study determined whether there are sex differences in the intrinsic passive mechanical properties of the MCA isolated from young, healthy male and female Sprague-Dawley (SD) rats and if they contribute to the differences in cerebral vascular function between sexes that may influence the onset and outcomes of CVD.

## MATERIALS AND METHODS

### Animals

All experiments were performed on 3-mo-male and female SD rats. The rats were bred in the colonies maintained at the University of Mississippi Medical Center (UMMC). All the animals housed under standard laboratory animal conditions, including a 12-h:12-h light-dark cycle with free access to food and water. The UMMC animal care facility is approved by the American Association for the Accreditation of Laboratory Animal Care. All protocols involving animals were approved by the Institutional Animal Care and Use Committees (IACUC) of the UMMC.

### Pressure Myography

**Isolation of the MCA.** Male and female SD rats were euthanized using 4% isoflurane. The rats were weighed, and the brains were collected and immediately placed in an ice-cold calcium-free physiological salt solution (PSS<sub>O<sub>Ca</sub></sub>), as we previously described (27). A 5 × 3 mm section from the brain containing the MCA was removed and placed in ice-cold PSS<sub>O<sub>Ca</sub></sub> supplemented with 1% bovine serum albumin (BSA). A branch-free M2 segment of the MCA with inner diameters (ID) ranging from 150 to 200 μm was dissected, as we previously described (26, 27).

**Myogenic reactivity.** Intact MCAs dissected from 11 male and 12 female SD rats were cannulated with glass pipettes in a pressure myograph chamber (Living System Instrumentation, Burlington, VT). The chamber was coupled to an inverted microscope (Olympus, Center Valley, PA) and bathed with 37°C oxygenated (21% O<sub>2</sub>-5% CO<sub>2</sub>-74% N<sub>2</sub>) PSS containing CaCl<sub>2</sub> (1.6 mM). Endothelial denudation was applied to the MCAs isolated from five male and five female SD rats by slowly perfusing 5–8 mL air through the lumen of the vessels, as described previously (10). The effective removal of the endothelium was validated by the elimination of the Acetylcholine-induced vasodilation (ACh; 10<sup>-8</sup> to 10<sup>-4</sup> mol/L). The MCA was equilibrated at an initial intraluminal pressure of 40 mmHg for 30 min to develop a spontaneous myogenic tone. The myogenic response was compared by measuring the IDs of the MCA in response to increased intraluminal pressures ranging from 40 to 180 mmHg in steps of 20 mmHg using a ×10 objective lens and imaged using a digital camera (MU1000, AmScope) as we previously described (26, 55).

**Passive mechanical properties of MCA.** After the myogenic reactivity was compared, the MCA was washed thoroughly with PSS<sub>O<sub>Ca</sub></sub> at 5 mmHg of intraluminal pressure. The outer and inner diameters (OD<sub>O<sub>Ca</sub></sub> and ID<sub>O<sub>Ca</sub></sub>) of the MCA were recorded under calcium-free conditions at 5 mmHg; then, the perfusion pressure was raised to 40 mmHg and then 180 mmHg in a 20-mmHg increment. The passive mechanical properties of the MCA including wall thickness (WT), cross-sectional area (CSA), wall-to-lumen ratio, distensibility, incremental distensibility, circumferential wall strain, circumferential wall stress, and myogenic tone were calculated at each transmural pressure step using the equations (see Fig. 5A) described previously (4, 9, 12, 20, 34, 38, 40, 59). The slopes (β-values) of the elastic modulus (stress-strain curves) were compared to determine the arterial stiffness. The β-value is directly proportional to the tangential or incremental elastic modulus obtained by fitting the stress-strain curves to an exponential model,  $y = \alpha e^{\beta x}$ , where  $y$  is circumferential stress,  $x$  is

the circumferential strain, and  $\alpha$  is the wall stress at the original diameter at 5 mmHg.

### Histology and Immunohistochemistry

**Sample selection and preparation for vascular smooth muscle cells and collagen.** Male and female SD rats were anesthetized with 2% isoflurane. The rats were weighed and perfused with 10% neutral-buffered formalin (Sigma-Aldrich, St. Louis, MO) intracardially at the perfusion pressure of 100 mmHg. The brains were collected and postfixed with 10% formalin. Two days later, a small rectangle square of brain tissue, ~4–5 mm in each length, containing the M1 and M2 segments of the MCA, was dissected and embedded with paraffin. We prepared 3-μm-thick serial cross sections encompassing the first 1–2 mm of the M2 segment of MCA. This segment of MCA displays a nearly uniform cylindrical shape. We systematically randomly sampled (SRS) a series of sections for stereology. The first section was randomly selected from the first 10 sections at the bifurcation point of the M1 to M2 segments of MCA and every 10th section thereafter. A total of six to eight sections of each animal was studied.

**Determination of the VSMC content in the wall of the MCA.** The VSMC content in the wall of the MCA was examined by immunofluorescent staining using an antibody against α-smooth muscle actin (α-SMA). Formalin-fixed and paraffin-embedded (FFPE) MCA sections were deparaffinized using xylene, followed by dehydration using a series of ethanol with decreasing concentrations. After being washed with deionized water, FFPE sections were incubated with proteinase K (S3020, Agilent, Santa Clara, CA) for 7 min for antigen retrieval. The sections were washed three times and incubated with the Protein Block Serum-Free Blocking (X0909, Agilent, Santa Clara, CA) for 1 h at room temperature, and followed by incubation with a primary antibody against mouse α-SMA (1:300, A5228, Sigma-Aldrich) and secondary antibody (goat anti-mouse Alexa Fluor 555, 1:1000, A21424, Thermo Fisher Scientific, Waltham, MA). The slides were then applied with a drop of an antifade mounting medium with DAPI (H-1200, Vector Laboratories, Burlingame, CA) and coverslipped. Images were obtained using a Nikon C2 laser scanning confocal on an Eclipse Ti2 inverted microscope (Nikon, Melville, NY) using a ×60 oil immersion objective and a ×3 digital zoom (total magnification of ×9,600). A series of optical sections were captured with a z step of 1.15 μm, and three images were used to generate a z-projection. Quantitation of α-SMA was determined by comparing the average intensities of the red fluorescence normalizing with CSA using NIS-Elements Imaging Software 4.6 (Nikon). The numbers of VSMCs determined by the distinct intercellular space between each cell were manually counted and normalized with CSA. All the images were taken using the same laser intensity, brightness, and contrast.

**Determination of the collagen content in the wall of the MCA.** Masson's trichrome staining was used to evaluate the collagen content in the wall of the MCA. Images were taken using a Nikon Eclipse 55i microscope and a DS-FiL1 color camera (Nikon). Quantitation of collagen in media and adventitial layers in the wall of the MCA was determined by comparing the average intensities of the blue staining using NIS-Elements Imaging Software 4.6 (Nikon).

**Determination of the elastin content in the wall of the MCA.** The elastin content in the wall of the MCA was determined using an approach described previously (34) based on the observation that a linear relationship exists between autofluorescence intensity and elastin content (5, 9). Briefly, a freshly isolated M2 of MCA was cannulated with glass pipettes in a pressure myograph chamber (Living System Instrumentation). After equilibration in PSS<sub>O<sub>Ca</sub></sub>, the vessels were fixed using 4% paraformaldehyde at 37°C at the perfusion pressure of 100 mmHg for 1 h. The vessels were incubated with 0.1 M sodium hydroxide at 75°C for 1 h to digest nonelastin components (9). The vessels were then removed from the pressure myograph and mounted in VECTASHIELD antifade mounting medium (H-1000, Vector Laboratories) on slides with a silicon spacer (500-μm

depth, 13-mm diameter; Grace Bio Laboratories, Bend, Oregon) to avoid compression.

Elastin autofluorescence was visualized, and images were captured at excitation and emission wavelengths of 488 nm and 500–560 nm, respectively (9, 34), using a Nikon C2 laser scanning confocal on an Eclipse Ti2 inverted microscope (Nikon) using a  $\times 60$  oil immersion objective,  $\times 3$  zoom (total magnification of  $\times 9,600$ ). A series of optical sections of each MCA at three to four different regions were imaged with a z step of 0.3  $\mu\text{m}$ , and a stack of three images, including all areas with intensive fluorescence, was compiled to generate a z-projection. Quantitation of elastin was determined by comparing the mean autofluorescence intensities per view using NIS-Elements Imaging Software 4.6 (Nikon). We also compared the thickness of internal elastic lamina (IEL), fenestrae numbers, and area per view. All the images were taken with the same laser intensity, brightness, and contrast.

#### Western Blot Analysis

The MCAs were isolated from male and female SD rats and homogenized in ice-cold radioimmunoprecipitation assay (RIPA, Sigma-Aldrich) buffer containing protease and phosphatase inhibitors (Thermo Fisher Scientific) using a ground glass homogenizer followed by using a bead-beating technology with a FastPrep-24 homogenizer (MP Biomedicals, Santa Ana, CA). Samples were transferred to a prechilled tube and sonicated on ice. The homogenate was centrifuged at 9,000 g for 15 min at 4°C. Protein concentration was determined by the Bradford method (Bio-Rad Laboratories, Hercules, CA). Aliquots of supernatant protein (10  $\mu\text{g}$  for  $\alpha$ -SMA and 30  $\mu\text{g}$  for elastin) were separated on a 10% SDS-PAGE gel and transferred to nitrocellulose membranes using a Trans-Blot Turbo Transfer System (Bio-Rad). Membranes were blocked with 5% nonfat milk at room temperature for 1 h and incubated with rabbit anti-elastin (1:200, ab217356, Abcam, Cambridge, MA) and mouse anti- $\alpha$ -SMA (1:1,000, A2547, Sigma-Aldrich) antibodies at 4°C overnight, followed by horseradish peroxidase (HRP)-conjugated goat anti-rabbit (1:5,000, ab6721, Abcam) and rabbit anti-mouse (1:20,000, ab97046, Abcam) secondary antibodies, respectively. The membranes were exposed to the SuperSignal West Dura substrate (Thermo Fisher Scientific), and the optical densities of bands were imaged and analyzed using a ChemiDoc Imager system (Bio-Rad). The membranes were then stripped and incubated with a rabbit anti-GAPDH antibody (1:1,000, 2118S, Cell Signaling Technology, Danvers, MA) followed by goat anti-rabbit (1:2,000, Cell Signaling) secondary antibody as a loading control.

#### CBF Responses

CBF responses to pressure and whisker stimulation in six male and seven female SD rats were compared following the protocol described previously (23, 24, 46). Briefly, the rats were anesthetized using ketamine (30 mg/kg) and inactin (50 mg/kg). This combination could maintain near-normal arterial pressure (110–120 mmHg) and has minimal effect on the autoregulation of CBF. The trachea was cannulated, and the animals were connected to a ventilator (SAR-830, CWE, Inc., Ardmore, PA).  $\text{CO}_2$  level was continually monitored and controlled at the range of 30–35 mmHg using an end-tidal  $\text{CO}_2$  Analyzer (CAPSTAR-100, CWE, Inc.). Cannulas were implanted in the femoral artery and vein for drug delivery and monitoring the mean arterial pressure (MAP). The head of the rat was fixed in a stereotaxic apparatus (model 900, David Kopf, Tujunga, CA), and the bone covering the left and right parietal bones (2 mm posterior and 6 mm lateral to the bregma) was thinned using a low-speed air drill until a thin translucent cranial window remained. A laser-Doppler flowmeter (LDF, PF5010, Perimed, Inc., Las Vegas, NV) probe was placed over the cranial windows in areas with no visible vessels in the field.

**Functional hyperemia.** Functional hyperemia was determined by measuring the CBF response to whisker stimulation using LDF. The

right whiskers were stimulated at 10 Hz for 60 s, as previously described (46). The LDF probe was immersed in the mineral oil on the left closed cranial window above the somatosensory cortex. Three trials were conducted every 5 min, and data were averaged for each experimental condition.

**Autoregulation of CBF.** Baseline CBF was recorded at 100 mmHg, followed by an elevation of blood pressure in steps of 20 mmHg up to 180 mmHg by infusing phenylephrine (0.5–5  $\mu\text{g}/\text{min}$ , P6126, Sigma-Aldrich) via the femoral vein. Blood pressure was maintained for 5 min at each step, and CBF was obtained when a steady-state CBF was achieved. Then, phenylephrine was withdrawn, allowing MAP to return to 100 mmHg, and a new baseline LDF signal was recorded. MAP was reduced to 40 mmHg in steps of 20 mmHg by graded hemorrhage, and CBF was obtained at each MAP level.

#### Cell Contraction Assay

**Isolation of cerebral vascular smooth muscle cells.** Primary cerebral VSMCs were isolated from 3-wk-old male and female SD rats, as described previously (26). The animals were euthanized using 4% isoflurane. The brains were collected, and the MCAs were dissected. The MCA was placed in ice-cold Tyrode's solution, PH 7.4. The MCA was cut into small pieces and incubated in low  $\text{Ca}^{2+}$  Tyrode's buffer, as we described previously (26) supplemented with dithiothreitol (2 mg/mL, Sigma-Aldrich) and papain (22.5 U/mL, Sigma-Aldrich) at 37°C for 15 min with gentle rotation. The MCA pieces were then pelleted at 1,000 RPM and resuspended in fresh Tyrode's solution containing trypsin inhibitor (10,000 U/mL, Sigma-Aldrich), collagenase (250 U/mL, Sigma-Aldrich), and elastase (2.4 U/mL, Sigma-Aldrich) with gentle rotation for 15 min at 37°C. The digested MCAs were centrifuged at 1,500 rpm for 10 min at 37°C, and the VSMCs were resuspended and released in Dulbecco's modified Eagle's medium (DMEM, Thermo Fisher Scientific) containing 20% fetal bovine serum and 1% penicillin/streptomycin. The cells were seeded into a CellTak (Thermo Scientific) precoated six-well plate, and early passages (P2-P3) of the primary VSMCs were used for following experiments.

**Cell constriction assay.** Cell contractile capability of male and female primary VSMCs isolated from SD rats was conducted using a collagen gel-based cell constriction assay kit (Cell Biolabs, San Diego, CA). The VSMCs were suspended in culture medium at a density of  $2 \times 10^6$  cells/mL, which was mixed with collagen gel working solution on the ice at a ratio of 1:4. The mixture at a final volume of 500  $\mu\text{L}$  containing  $2 \times 10^5$  cells was placed in each well of 24-well plate and incubated at 37°C for 1 h, and then, 1 mL culture medium was gently added to each collagen gel. The cells were further incubated 2 days at 37°C in a 5%  $\text{CO}_2$  atmosphere to develop contractile stress. The stressed matrix was detached from the wall using a sterile needle to initiate contraction. Changes in the collagen gel size were imaged before (*time 0*) and 120 min after additional stimulation at 30-min interval and quantified with NIS-Elements Imaging Software 4.6 (Nikon).

#### Eight-Arm Water Maze

Spatial learning and short- or long-term memory were compared with an eight-arm radial water maze (57). The rats were placed in the testing room 2 h before training to equilibrate to the new environment. The rats were trained to recognize the platform located in one of the eight arms on the morning of the first day, and four + four trials were conducted 2 and 24 h posttraining, respectively. Time to reach the platform was recorded.

#### Statistics

All data are presented as mean values  $\pm$  SE. A two-way ANOVA for repeated measures followed by a Holm-Sidak post hoc test was used to compare the significant differences between male and female

SD rats in corresponding values in the pressure myograph studies. The significance of differences between groups in corresponding values of MAP, body weight, cell contraction assay, Western blot, and immunohistochemistry was compared using Student's *t* test. The stress-strain curves were fitted using the Levenberg-Marquardt regression method (linear and nonlinear regressions), and the slopes were compared by using Student's *t* test. All statistical analyses were performed using GraphPad Prism 6 (GraphPad Software, Inc., La Jolla, CA). A value of  $P < 0.05$  was considered significant.

## RESULTS

### *Sex Differences in MAP, Body, and Brain Weights*

As demonstrated in Fig. 1, 3-mo-old female SD rats have significantly lower MAP, body, and brain weights ( $101.0 \pm 1.5$  mmHg,  $214.4 \pm 7.6$  g, and  $1.68 \pm 0.02$  g, respectively) compared with age-matched male SD rats ( $120.8 \pm 4.3$  mmHg,  $380.6 \pm 13.8$  g, and  $1.97 \pm 0.03$  g, respectively).

### *Sex Differences in the VSMCs Content in the Wall of the MCA*

Differences in VSMCs content were determined by immunofluorescence staining using an antibody  $\alpha$ -SMA. We found that there were fewer VSMC layers in the wall of the MCA in female rats (Fig. 2A). The numbers of VSMCs/mm<sup>2</sup> were 4% less in the MCA of females compared with males (Fig. 2B). The average fluorescent intensity/ $\mu$ m<sup>2</sup> was decreased by 18% in the MCA of female versus male rats (Fig. 2C). The expression of  $\alpha$ -SMA in isolated MCAs was significantly decreased in females compared with males examined by Western blot (Fig. 2, D and E).

### *Sex Differences in the Collagen Content in the Wall of the MCA*

Masson's trichrome staining was used to determine sex differences in the collagen content in the wall of the MCA (Fig. 3). We found that average blue intensity, stained by methyl blue that is collagen specific, was significantly increased in the tunica media but did not display significant differences in the tunica adventitia in the wall of the MCA of females compared with men.

### *Sex Differences in the Elastin Content in the Wall of the MCA*

Sex differences in the elastin content in the wall of the MCA estimated by confocal microscopy are presented in Fig. 4. Consistent with the previous report (44), we found that the external elastic lamina was absent in rat MCA in both sexes. IEL thickness was thicker in the MCA in females (Fig. 4A) in association with higher autofluorescence intensity (Fig. 4, B and E), smaller fenestrae areas (Fig. 4, C and E), and fewer number of fenestrations (Fig. 4, D and E). The expression of elastin in isolated MCAs was significantly increased in females compared with males examined by Western blot (Fig. 4F).

### *Sex Differences in Vascular Characteristics of the MCA*

Figure 5 presents the vascular characteristics of the MCA isolated from 3-mo-old male and female SD rats. ID<sub>0Ca</sub> of the MCA was similar in male and female rats at 5 mmHg of intraluminal pressure but were smaller in females at perfusion pressures from 40 to 180 mmHg (Fig. 5B). WT and CSA of MCA were smaller in female versus male rats at intraluminal pressures from 5 to 180 mmHg (Fig. 5, C and D), but the wall-to-lumen ratio was lower only at a pressure of 5 mmHg (Fig. 5E).

### *Sex Differences in the Myogenic Response and CBF Autoregulation of the MCA*

The MCA of male and female SD rats displayed a similar vasoconstrictive response to increases in perfusion pressure from 40 to 120 mmHg. In contrast, female vessels failed to constrict and exhibited forced dilation over the pressure range of 140–180 mmHg. The female MCA was 16% larger at 180 mmHg in comparison with males (Fig. 6A). There was no significant difference in the myogenic response between endothelium-intact MCA and endothelium-denuded MCA in both male and female SD rats (Fig. 6A). As depicted in Fig. 6B, there was no significant difference in CBF autoregulation in male and female SD rats when blood pressures were in the range from 40 to 140 mmHg. However, females, but not males, exhibited autoregulatory breakthrough at blood pressure greater than 140 mmHg. CBF increased by  $57.4 \pm 4.4\%$  in females versus  $30.1 \pm 3.1\%$  in males, respectively, at a perfu-

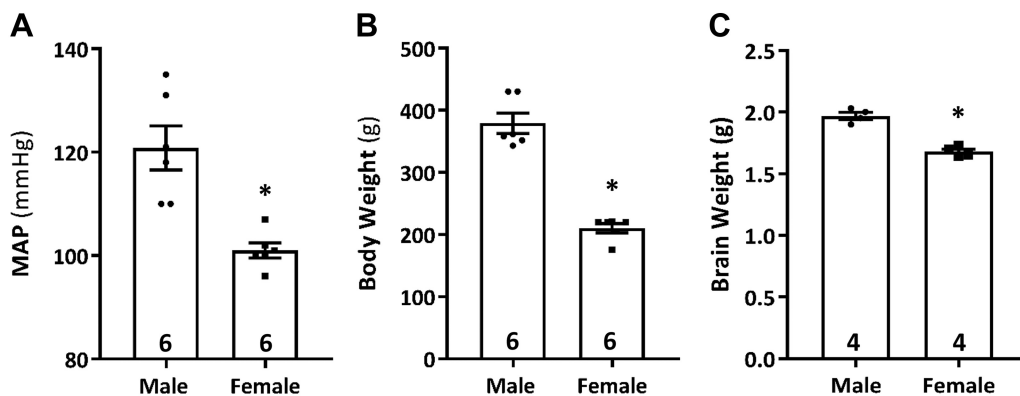


Fig. 1. Sex differences in mean arterial pressure (MAP), body, and brain weights. A: comparison of MAP in 3-mo-old male and female Sprague-Dawley (SD) rats. B: comparison of body weight in 3-mo-old male and female SD rats. C: comparison of brain weight in 3-mo-old male and female SD rats. Mean values  $\pm$  SE are presented. Numbers indicate the number of animals studied per group. \* $P < 0.05$  from the corresponding values in female vs. male SD rats.

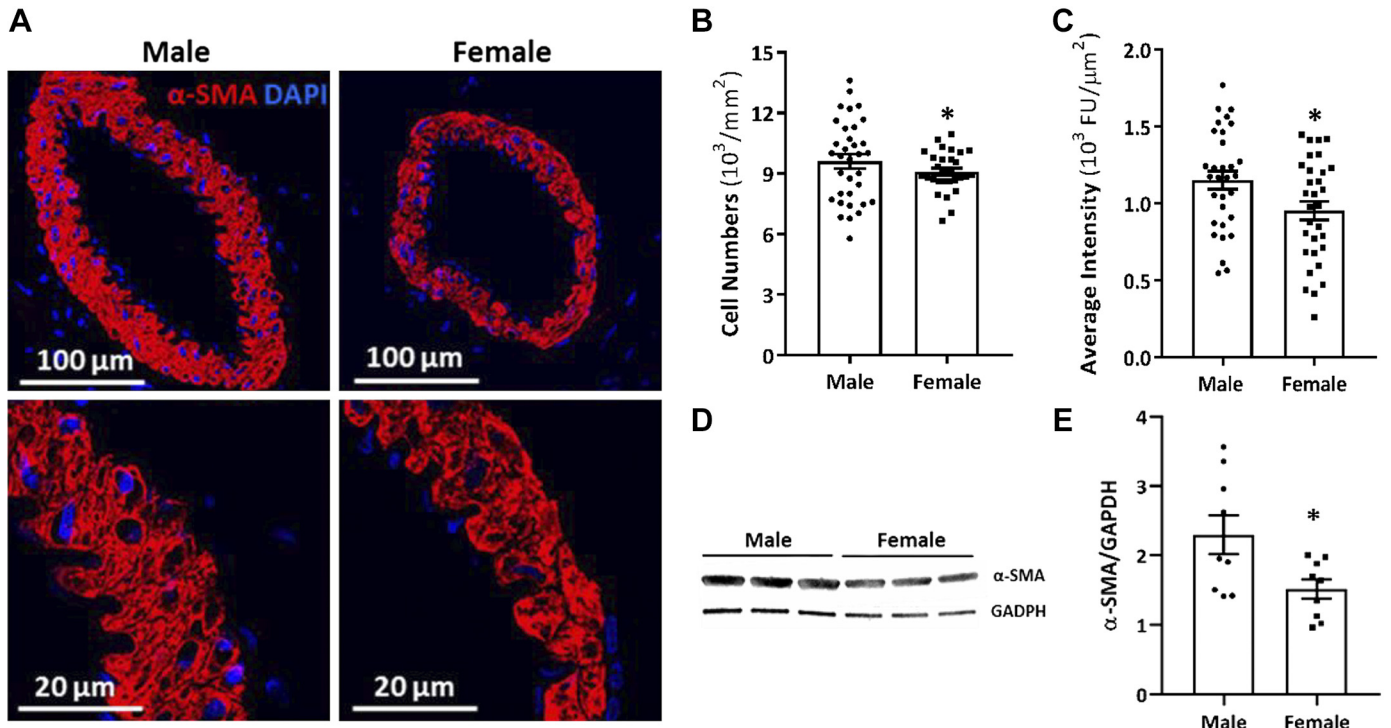


Fig. 2. Sex differences in the VSMC content in the wall of the middle cerebral artery (MCA). *A*: representative images of immunofluorescence staining of  $\alpha$ -smooth muscle actin ( $\alpha$ -SMA) in the wall of the MCA of male and female Sprague-Dawley (SD) rats. *B*: comparison of VSMC numbers of cell/mm<sup>2</sup> cross section the wall of the MCA of male and female SD rats. *C*: comparison of the red average fluorescent intensity [fluorescence unit (FU)]/ $\mu$ m<sup>2</sup> in the wall of the MCA of male and female SD rats. *D* and *E*: representative images of Western blot and quantification of the expression of  $\alpha$ -SMA in isolated MCAs of male and female SD rats. Mean values  $\pm$  SE are presented. Five male and five female rats were used for immunofluorescent staining. For Western blot, protein samples were extracted from 7 male and 5 female rats. The protein was pooled in each sex, and triplets were used in each experiment. Experiments were repeated 3 times. Each dot represents 1 view or 1 of the triplets, but average numbers obtained in each rat was used for statistical analysis. \* $P < 0.05$  from the corresponding values in female rats vs. male rats.

sion pressure of 180 mmHg. These results indicate that female SD rats have a reduced range of CBF autoregulation compared with age-matched males in response to higher pressures.

#### Sex Differences in Cerebral VSMC Contractile Capability

The effects of sex differences in cerebral VSMC contractile capability are presented in Fig. 6C. The VSMCs isolated from female cerebral vasculature exhibited a weaker contractile

capability, and the gel size was reduced by  $26.0 \pm 0.4\%$  versus  $31.9 \pm 0.5\%$  in cells isolated from men.

#### Sex Differences in Mechanical Properties of the MCA

The MCA of females exhibited less distensibility at perfusion pressures from 40 to 180 mmHg (Fig. 7A), and lower incremental distensibility at perfusion pressures from 40 to 100 mmHg (Fig. 7B). Female MCA had more wall stress at perfu-

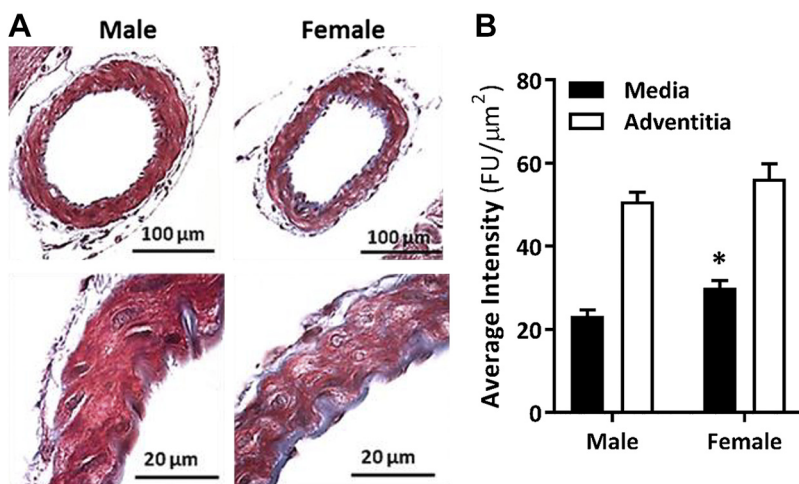


Fig. 3. Sex differences in the collagen content in the wall of the middle cerebral artery (MCA). *A*: representative images of the comparison of sex differences in the collagen content in the wall of the MCA using Masson's trichrome staining. *B*: comparison of the average blue intensity [fluorescence unit (FU)]/ $\mu$ m<sup>2</sup> cross-section area in the tunica media and adventitia of the MCA of male and female Sprague-Dawley (SD) rats. Mean values  $\pm$  SE are presented. Five male and five female rats were studied. \* $P < 0.05$  from the corresponding values in female rats vs. male rats.

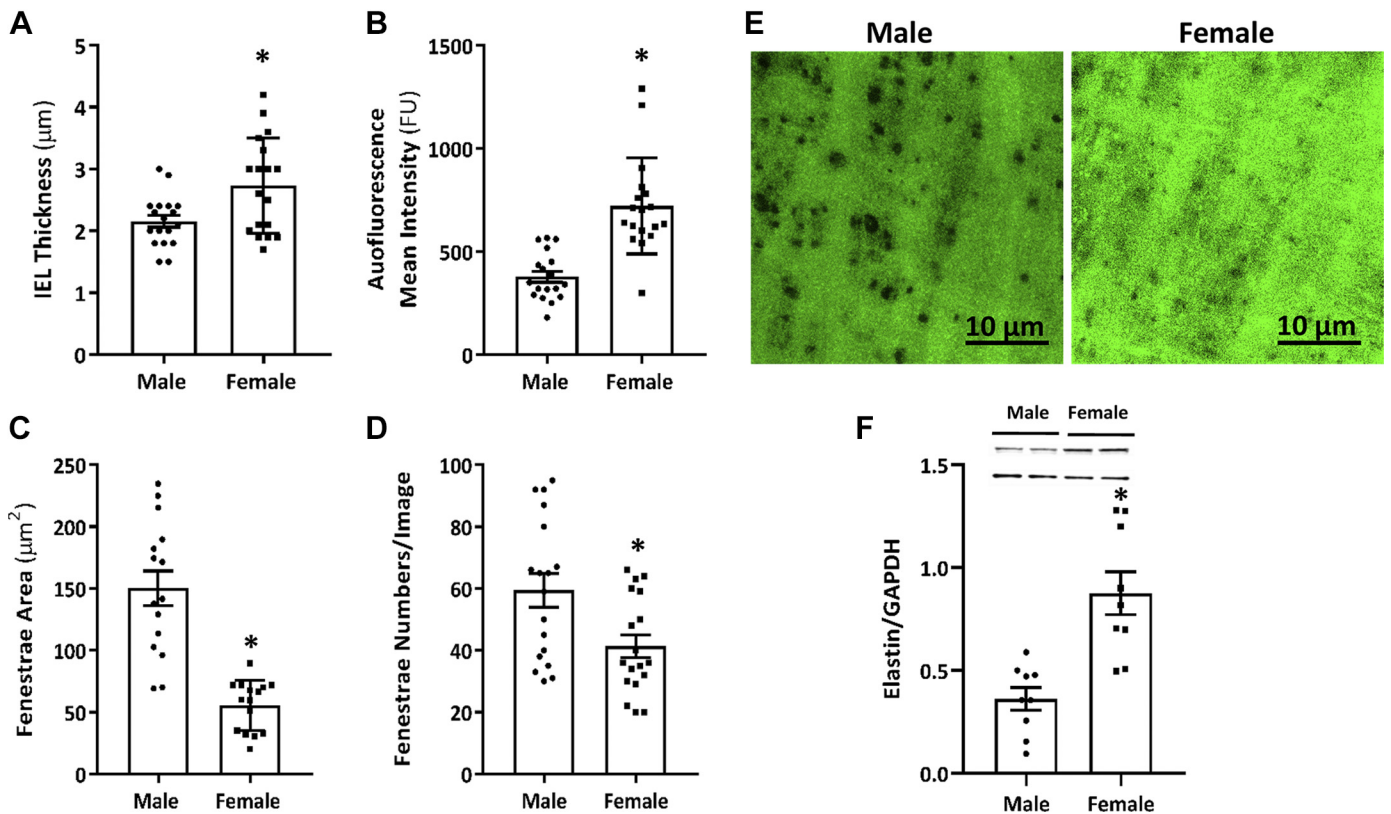


Fig. 4. Sex differences in the elastin content in the wall of the middle cerebral artery (MCA). *A*: comparison of internal elastic lamina (IEL) thickness in the MCA of male and female Sprague-Dawley (SD) rats. *B*: comparison of the autofluorescence intensity [fluorescence unit (FU)] in the IEL on the MCA of male and female SD rats. *C*: comparison of the fenestrae areas in the IEL on the MCA of male and female SD rats. *D*: comparison of the fenestrae numbers in the IEL on the MCA of male and female SD rats. *E*: representative images of the elastin autofluorescence in the IEL detected by confocal microscopy. *F*: representative images of Western blot and quantification of the expression of elastin in isolated MCA of male and female SD rats. Mean values  $\pm$  SE are presented. Five male and five female rats were used for the detection of elastin autofluorescence. For Western blot, protein samples were extracted from 7 male and 5 female rats. The protein was pooled for each sex, and triplets were used in each experiment. Experiments were repeated 3 times. Each dot represents 1 view or 1 of the triplets, but average numbers obtained from each rat were used for statistical analysis. \* $P < 0.05$  from the corresponding values in female rats vs. male rats.

sion pressures from 40 to 180 mmHg (Fig. 7C). The stress-strain curves of MCA shifted to the left in females compared with males (Fig. 7D). The  $\beta$ -values (Fig. 7E), the indicator of vascular stiffness, were significantly increased in the MCA of females ( $10.0 \pm 0.7$ ) than males ( $7.4 \pm 0.7$ ). The MCA developed a more myogenic tone in females at the perfusion pressures ranging from 40 to 120 mmHg (Fig. 7F). However, there was no significant difference in the myogenic tone between male and female SD rats when perfusion pressure was increased further to 140–180 mmHg.

A summary of the sex differences in vascular characteristics of the MCA at a perfusion pressure of 100 mmHg is presented in Fig. 7G. At calcium-free conditions, the MCA of female SD rats displayed smaller  $ID_{0ca}$ ,  $OD_{0ca}$ , WT, and CSA, but there were no changes in the wall-to-lumens ratio. The MCA of female SD rats had less distensibility and incremental distensibility. However, they exhibited higher myogenic tone and wall stress under the same perfusion pressure.

#### Sex Differences in Functional Hyperemia and Cognitive Function

The time course of changes in cortical CBF in response to whisker stimulation is presented in Fig. 8A. The average of CBF increased during the 60-s stimulation period was to the

same extent in females (by  $30.3 \pm 1.4\%$ ) versus male (by  $29.2 \pm 3.3\%$ ) SD rats.

The females took the same time to escape from an eight-arm water maze compared with males (Fig. 8B), indicating there were no significant differences in spatial learning and memory function in these rats at a young age.

#### DISCUSSION

CVD is the leading cause of dementia and death among middle-aged and elderly adults globally (13, 72, 78). Men and women display profound divergence in the onset, progression, and outcomes of CVD (16). Young women are protected from CVD throughout adulthood but are at higher risk than men after menopause (30, 62, 66). Indeed, the changes in sex hormones with age in women are essential factors contributing to the differences in cerebral vascular protection in women; however, hormone replacement therapy does not reduce CVD risk in postmenopausal women (69, 79). In addition, women have a longer life span. When superimposing with hypertension, diabetes, and atrial fibrillation, postmenopausal women have higher CVD risk and more negative outcomes than age-matched men (33). Current pharmacological interventions cannot prevent and do not reduce the increased risk of CVD in postmenopausal women, suggesting a better understanding of

## A

Parameter	Formulas
Wall thickness ( $\mu\text{m}$ )	$WT = (OD_{0Ca} - ID_{0Ca}) / 2$
Cross-sectional area ( $\mu\text{m}^2$ )	$CSA = (\pi/4) \times (OD_{0Ca}^2 - ID_{0Ca}^2)$
Wall/lumen	$(OD_{0Ca} - ID_{0Ca}) / 2ID_{0Ca}$
Myogenic tone (%)	$(ID_{0Ca} - ID_{Ca}) / ID_{0Ca} \times 100$
Distensibility (%)	$(ID_{0Ca} - ID_{0Ca5mmHg}) / ID_{0Ca5mmHg} \times 100$
Incremental distensibility (%/mmHg)	$\Delta ID_{0Ca} / (ID_{0Ca} \times \Delta P) \times 100$
Circumferential wall strain	$\epsilon = (ID_{0Ca} - ID_{0Ca5mmHg}) / ID_{0Ca5mmHg}$
Circumferential wall stress ( $\times 10^6$ dynes/cm <sup>2</sup> )	$\sigma = (P \times ID_{0Ca}) / (2WT)$

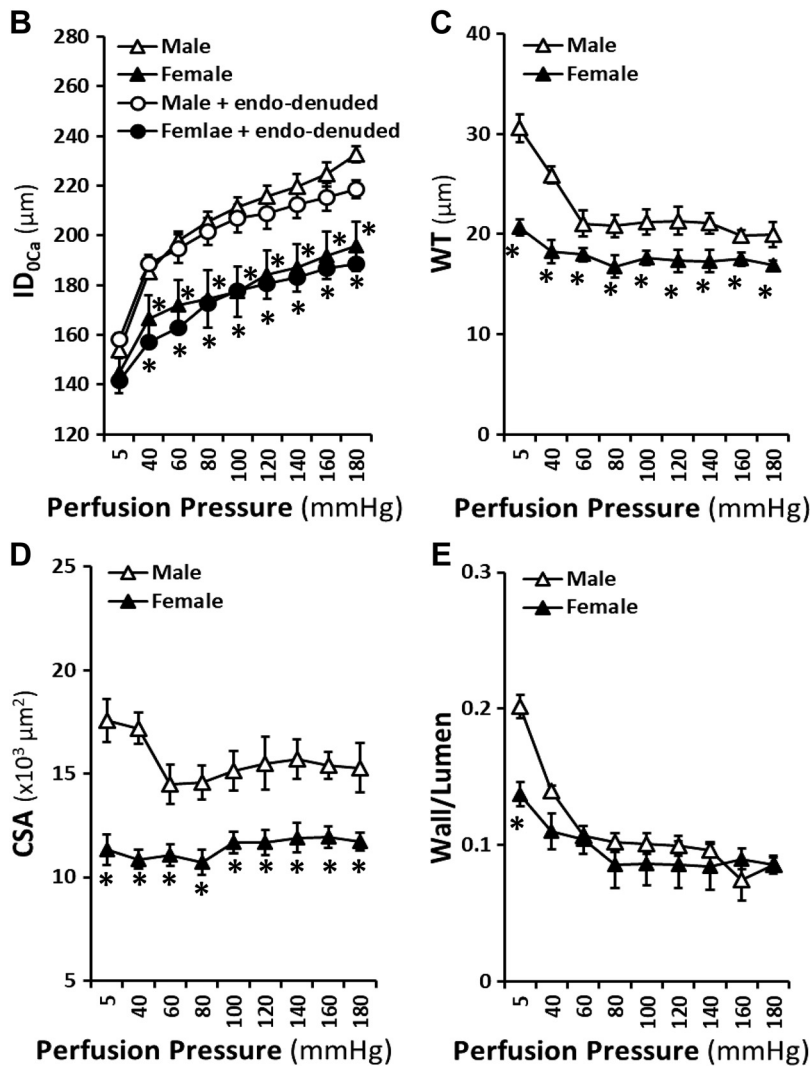


Fig. 5. Sex differences in vascular characteristics of the middle cerebral artery (MCA). *A*: Equations used for the calculation of vascular mechanical properties.  $ID_{Ca}$ , inner diameter in  $Ca^{2+}$  solution;  $ID_{0Ca}$ , inner diameter in  $Ca^{2+}$  free solution;  $OD_{0Ca}$ : outer diameter in  $Ca^{2+}$  free solution;  $ID_{0Ca5mmHg}$ , inner diameter in  $Ca^{2+}$  free solution at a pressure of 5 mmHg;  $P$ , perfusion pressure, 1 mmHg = 1,334 dyne/cm<sup>2</sup>. *B*: comparison of  $ID_{0Ca}$  of endothelium-intact and endothelium-denuded MCA isolated from 3-mo-old male and female Sprague-Dawley (SD) rats. *C*: comparison of the wall thickness (WT) of MCA of male and female SD rats. *D*: comparison of the cross-sectional areas (CSA) of MCA of male and female SD rats. *E*: comparison of the wall-to-lumen ratios of MCA of male and female SD rats. Mean values  $\pm$  SE are presented. Six male and seven female rats were studied using endothelium-intact MCA. Five male and five female rats were studied using endothelium-denuded MCA. \* $P < 0.05$  from the corresponding values in female vs. male rats.

sex differences in structure and function of the cerebral vasculature is needed to determine the underlying mechanisms.

In the present study, we compared the intrinsic structure, the proportional composition, passive distensibility, and stiffness of MCA; myogenic reactivity in response to elevations in transmural pressure; functional hyperemia and autoregulation of CBF in vivo; as well as cognitive function using age-matched young, healthy male and female SD rats. We found that first, female SD rats at 12-wk of age exhibited lower

MAP, body, and brain weights compared with age-matched males. Second, the MCA dissected from female SD rats displayed fewer VSMCs and more collagen in the media of the vascular wall in associated with a thicker IEL. Third, VSMCs of females exhibited a weaker contractile capability. Fourth, wall thickness and the inner diameter of the MCA were smaller in females. 5) Fifth, female MCA had a greater myogenic tone and wall stress but less distensibility. Sixth, female MCA had reduced constrictive responses to elevations in perfusion pres-

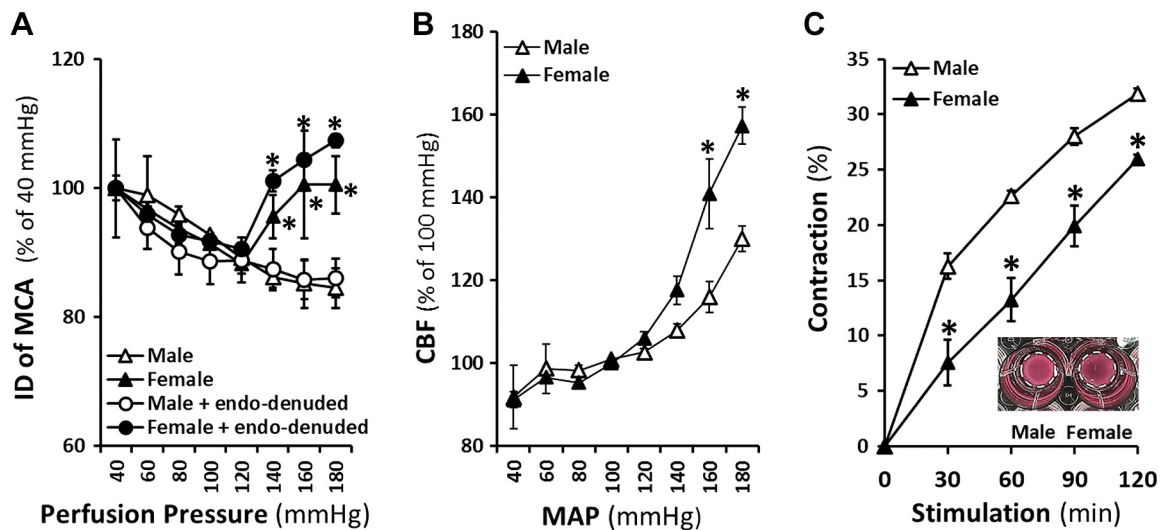


Fig. 6. Sex differences in the myogenic response of the middle cerebral artery (MCA), cerebral blood flow (CBF) autoregulation, and cerebral VSMC contractile capability. *A*: comparison of the myogenic response of MCA of female vs. male Sprague-Dawley (SD) rats in response to an elevation in perfusion pressure. *B*: the relationships of CBF and mean arterial pressure (MAP) were compared in male and female SD rats. *C*: comparison of sex differences in cerebral VSMC contractile capability as of %constriction to initial size is presented. Representative images are shown in the inset. The white dotted circles represent the gel area. Mean values  $\pm$  SE are presented. Cerebral VSMCs were isolated from 6 male and 6 female rats. The cell contraction experiments were repeated 3 times, and triplicates were used in each experiment. \* $P < 0.05$  from the corresponding values in female vs. male rats.

sure *ex vivo* (myogenic response) and *in vivo* (CBF autoregulation). Forced dilation of the MCA occurred at pressures  $>140$  mmHg in females, which mediated autoregulatory breakthrough at high pressures. Seventh, the removal of the endothelium in the MCA did not alter the myogenic response in both males and females. Eighth, we did not find sex differences in functional hyperemia and cognitive function.

We took into account the fact that several factors could influence the results. First, we compared the wall structure and components using the same M2 segments of MCA as for the measurements of myogenic reactivity. Second, we performed perfusion fixation of the MCA with 10% neutral-buffered formalin in calcium-free PSS solution at 100 mmHg to mimic the *in vivo* blood pressure of these rats. Third, we systematically randomly sampled (SRS) series of 3  $\mu$ m thick sections encompassing the first 150  $\mu$ m of M2 segment from the bifurcation point of the M1 segment of the MCA where the vessels are nearly uniformly cylindrical. The first section was randomly selected from the first 10 sections of the bifurcation point of M1 to M2 segments of MCA, and six to eight subsequent sections from each animal were studied. Fourth, we compared VSMCs and collagen content in the tunica media layer of the arterial wall, which are the main active elements to determine the passive mechanical properties of arteries (20). We also compared elastin in the tunica intima layer and collagen in the tunica adventitia layer. Finally, we did not monitor the estrous cycle in females in this study based on several considerations: 1) we did not find any differences in the myogenic response and CBF autoregulation in another study at various stages in the estrous cycle (82); 2) recent studies demonstrated that the effects of the estrous cycle on 142 cardiovascular phenotypes were much less than sex differences (17); 3) CBF autoregulation is unaffected by cycle in young females (28); and 4) the rats used in this study were bred in the colonies maintained at our institution. Females were group-housed since birth, which can reach cycle synchronously (49).

VSMCs provide structural integrity and mediate the diameter changes in response to stimulation. In rats, VSMC is the most abundant cell type that occupies up to 73% in cerebral arteries of 25-wk-old male Wistar-Kyoto (WKY) rats (7) and 65% at 10-mo-old age (4). These results suggest that the number of cerebral VSMCs may decrease with age in rats, which is consistent with other studies in mice indicating the myogenic response and autoregulation of CBF are impaired with age, especially when superimposed with hypertension (75, 76). A significant intrinsic property of VSMCs is the myogenic response, which constricts the vessels in response to elevations in intraluminal pressure (22). VSMCs dynamically regulate the diameter of the vessels by constricting and relaxing in response to stimuli, such as vasoconstrictors, stretch, vasodilators, and metabolic factors. Under pathological conditions, these cells can migrate and proliferate that play essential roles in vascular inflammation and atherosclerosis (50). Interestingly, we found that there are more layers of VSMCs in the wall of MCA in males than in females. This result is consistent with less  $\alpha$ -SMA expression in isolated MCAs in females than males using Western blot analysis. The female MCA exhibited a thinner wall and smaller CSA, a narrower lumen than males. However, the wall-to-lumen ratio was the same between the two sexes.

Elastin in the vascular wall stabilizes the arterial structure and endows vessels with elasticity (41, 68). IEL and endothelial cells make up the intima. In the media, elastin is organized in sheets (lamellae) with collagen, VSMCs, and extracellular matrix (ECM) (80). Rats cerebral arteries lack the external elastic lamina, which is similar to humans (44). Elastin is autofluorescent, and a linear relationship exists between fluorescence intensity and elastin content (9). Based on this relationship, we found there were fewer fenestrations of elastin in the IEL of MCA of females in comparison with males. This result is consistent with our finding of more elastin expression in isolated MCAs from females using Western blot analysis.



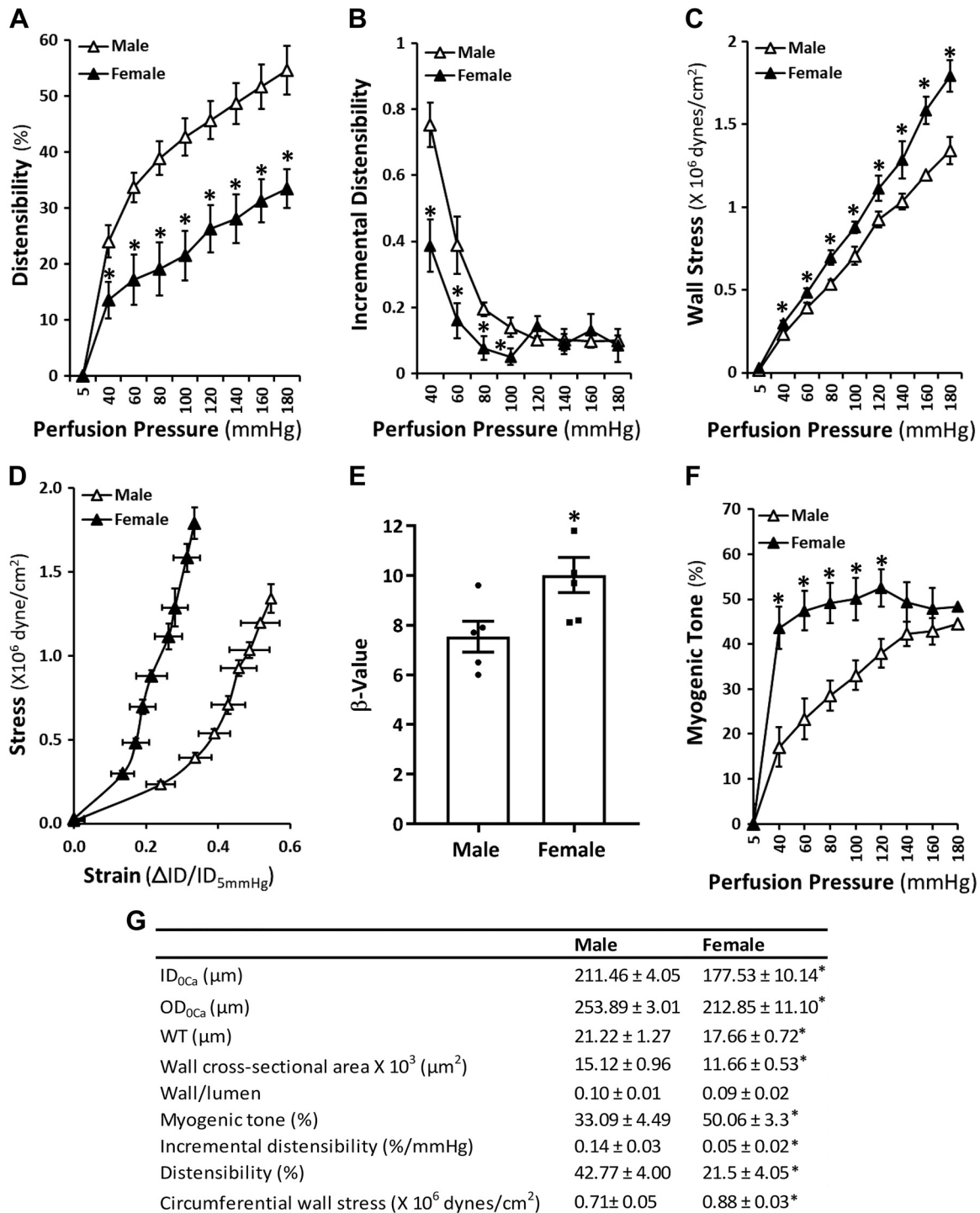


Fig. 7. Sex differences in mechanical properties of the middle cerebral artery (MCA). *A*: comparison of the distensibility of the MCA of female vs. male Sprague-Dawley (SD) rats. *B*: comparison of the incremental distensibility of the MCA of female vs. male SD rats. *C*: comparison of the wall stress of the MCA of female vs. male SD rats. *D*: comparison of the stress-strain relationships of the MCA of female vs. male SD rats. *E*: comparison of the slopes of the elastic modulus curves ( $\beta$ -values) of the MCA of female vs. male SD rats. *F*: comparison of the myogenic tone of the MCA of female vs. male SD rats. *G*: comparison of sex differences in vascular characteristics of the MCA at a perfusion pressure of 100 mmHg. All data are presented as mean values  $\pm$  SE. Six male and seven female rats were studied. \* $P < 0.05$  from the corresponding values in female vs. male rats.

Fenestrations in IEL of cerebral arteries and other resistant arteries exist in rodents (9, 60, 63) and other mammals (36). The size of fenestrations is increased from birth to middle age in humans and rodents and followed a gradual decline with aging (34, 44). However, fenestration size and the fraction of

area were smaller in resistant vessels of stroke-prone spontaneously hypertensive rat (SP-SHR) (6) and spontaneously hypertensive rat (SHR) (63) than WKY rats. Clinical studies indicated the function of elastin in cerebral arteries declined with aging, although the fraction remained unchanged (29).

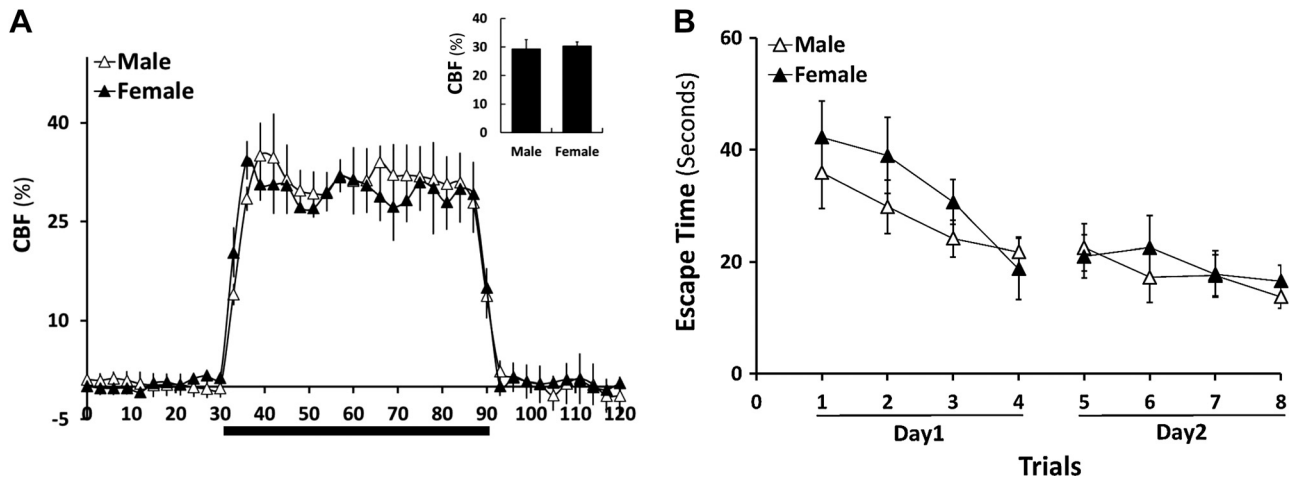


Fig. 8. Sex differences in functional hyperemia and cognitive function. *A*: Comparison of functional hyperemia responses of female vs. male Sprague-Dawley (SD) rats as presented as a time course of percentage changes of cortical cerebral blood flow (CBF) in response to whisker stimulation. Averaged percentage changes in CBF during 60 s stimulation are presented as the inserted graph. *B*: Comparison of cognitive function of female vs. male SD rats determined using an eight-arm water maze. All data are presented as mean values  $\pm$  SE. Six male and seven female rats were studied.

Collagen is a reinforcing structural element and the major nondistensible component in the arterial wall. Within the media, it surrounds the vessels in a helical shape, and this structural arrangement, along with elastin and VSMCs, is responsible for maintaining the structural integrity of the vessels as well as its distensibility or lack thereof. In the adventitia, collagen is arranged longitudinally along the vessel wall and markedly contributes to vascular stiffness and compliance (80). Our results demonstrated that there was markedly more collagen content in the media but not the adventitia of MCA in females in comparison with males.

Indeed, chronic hypertension in some models promotes hypertrophic remodeling and reduces the distensibility of cerebral arteries in association with increased collagen content in the vascular wall (3, 39). In the present studies, we found that 3-mo-old female SD rats had a significantly lower MAP compared with age-matched men; however, the MAPs in females ( $101.0 \pm 1.5$  mmHg) and males ( $120.8 \pm 4.3$  mmHg) were within the normotensive range. Thus, we think the structural and functional alterations we observed between male and female SD rats were not induced by the small difference in MAP.

This sexual dimorphism in the intrinsic structure of the MCA would be expected to alter the myogenic reactivity and passive mechanical properties between males and females. Indeed, we found that basal myogenic tone was enhanced in female MCA. This observation is consistent with previous findings (54). However, the molecular and cellular mechanisms involved in the increased tone are still unclear. Estrogen enhances the production of NO and other vasodilators (31, 56), which would be expected to reduce myogenic tone. On the other hand, female MCA has a greater response to NO, a lower response to ANG-II and ET-1, and no response to thromboxane A<sub>2</sub> agonists (1, 43). Many other factors that contribute to the regulation of cerebral vascular function have been reported, such as peroxisome proliferator-activated receptor- $\gamma$  (11), estrogen receptors (86), transient receptor potential channels, integrins, and actin cytoskeletal dynamics that involving activation of protein kinase C, mitogen-activated protein kinases,

and RhoA-Rho kinase pathways, etc. (22, 25), may all play roles in the enhanced basal vascular tone in females as we observed in our studies. Clearly, more in-depth investigations are needed to determine the causes and functional consequences of elevated tone in females. The incremental distensibility and circumferential wall strain were reduced in female MCA relative to males. Females exhibited more circumferential wall stress, a leftward shift of the elastic modulus (stress-strain curves) indicating less distensibility, and larger  $\beta$ -values, which were calculated from the elastic modulus using an exponential model and directly proportional to tangential elastic modulus as an indicator of intrinsic stiffness independent of geometry (58, 60). The parameters in female MCA compared with male MCA are similar to the difference in the myogenic and structural properties of the MCA in SP-SHR versus SHR (40). The MCA in SP-SHR has a smaller passive lumen diameter, reduced distensibility, a leftward shift stress-strain relationship, but an increased vascular wall thickness. These structural changes are associated with an increased incidence of hemorrhagic stroke in this strain.

It is logical to expect that a stiffer and less distensible vessel in females constricts less in response to elevations in perfusion pressure, as demonstrated in our results. Although female MCA exhibited higher responses to hypercapnia, NO, and flow-mediated vasodilation (31, 47, 54, 56), we found that removal of endothelial cells in MCA had no effects on the myogenic response in both sexes, indicating endothelial cells did not play a significant role in the reduced pressure-induced vascular reactivity in females. This finding is consistent with previous reports that the myogenic responses were independent of the endothelium in both human and rat cerebral resistant arteries (48, 81). The myogenic response is mainly determined by VSMCs within the tunica media layer. Stretch-activated ion channels on the VSMCs are the mechanosensors allowing Ca<sup>2+</sup> influx to induce vasoconstriction (32, 84). Calcium-activated K<sup>+</sup> channels are a negative feedback mechanism resulting in VSMCs membrane hyperpolarization and reduced vasoconstriction (8, 53). A recent study indicated that VSMCs isolated from MCAs of adult female rats exhibited higher BK

channel current densities compared with males leading to attenuated myogenic reactivity (61). In addition, a higher basal vascular tone would be expected to blunt subsequent myogenic responses (53). In addition to fewer VSMCs in the MCA wall in females, we found that at a given number, primary VSMCs isolated from female MCA had less contractile capability than VSMCs of male MCA. These factors led to a diminished myogenic response in female MCA in association with an attenuated CBF autoregulation, as demonstrated in our results. CBF autoregulation is mainly regulated by the myogenic response. Female vessels exhibited a forced dilation of the MCA and an autoregulatory breakthrough at pressures above 140 mmHg. The increased slope of the CBF autoregulation curve at high pressures in females is likely affected by the reduced myogenic response but unlikely due to decreased distensibility of the MCA. Autoregulation of CBF is critical for brain homeostasis to maintain constant blood flow despite changes in systemic pressure (65). Impaired autoregulation of CBF and the myogenic response of the large cerebral arteries and arterioles can increase transmission of pressure to downstream small arterioles and capillaries, leading to microhemorrhages, blood-brain barrier leakage, and ischemic injury in various pathologic conditions (21, 23, 24, 83).

At first glance, our results are controversial with others that females have better autoregulation than males at all ages (19, 28). This discrepancy is primarily due to differences in the experimental design and methods used in these studies. We measured the CBF in response to changes in blood pressure, while human studies examined the ability to maintain CBF at given (physiological) pressure in response to elevated, inspired CO<sub>2</sub> or postural changes (19, 28). These studies thus showed that women were better able to dilate the cerebral circulation and maintain CBF under these conditions compared with men

but did not have evidence that women have better “autoregulation” in response to fluctuation of pressure changes. Another consideration is that we assessed CBF by transcranial Doppler measurements of blood flow velocity in the pial arteries. The missed link between smaller vessels, less compliance, elevated tone, reduced the myogenic response, and attenuated CBF autoregulation to higher CBF in female MCA could be explained that women had elevated basal flow velocities in the MCA examined in 304 healthy men and women (42) and enhanced flow velocity under hypercapnia condition were found higher in women (47, 54).

Functional hyperemia mediated by neurovascular coupling mechanisms is essential in regulating CBF in response to neuronal activities and is independent of changes in blood pressure (2, 14, 15, 18, 73). Endothelial cells, pericytes, and astrocytes play a critical role in functional hyperemia (74). We found that functional hyperemia responses to whisker-barrel stimulation were not different between males and females, which is consistent with recent human studies (71). In addition, the differences in the structure and function of the MCA did not induce subsequent pathological effects on cognitive function examined with eight-arm water maze in females.

In summary (Fig. 9), our results demonstrated that the MCA of female SD rats exhibits more elastin expression in association with a thicker IEL with smaller fenestrae areas and fewer fenestrae numbers compared with the MCA of males. In the media layer of the MCA, females had less VSMCs and more collagen contents. Primary VSMCs isolated from female MCA had diminished contractile capability than males. We found that female rats had a thinner vascular wall and a smaller inner diameter of the MCA compared with males but had no changes in the wall-to-lumen ratio. Female MCA developed higher basal myogenic tone, lower distensibility, and higher wall

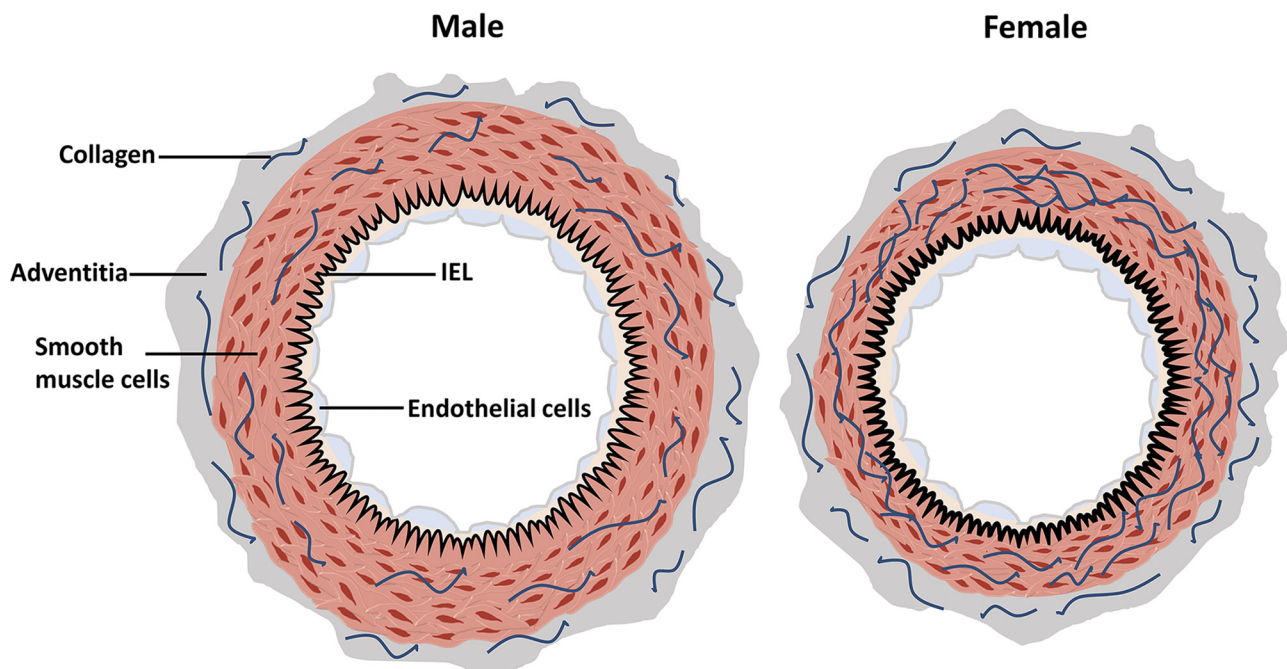


Fig. 9. Summary of the fundamental structural differences in the M2 branch of the middle cerebral artery (MCA) between sexes. MCA of female rats has a smaller inner diameter, thinner wall, less VSMCs and more collagen in the tunica media, and a thicker internal elastic lamina under calcium-free conditions compared with men. IEL, internal elastic lamina.

stress in association with less myogenic response and CBF autoregulation compared with males. The structural differences did not alter neurovascular coupling responses and cognition at a young age; however, they might play a role in the development of CVD after menopause or in hypertension.

#### GRANTS

This study was supported by National Institutes of Health Grants AG-050049, AG-057842, P20-GM-104357, and HL-138685 and American Heart Association Grants 16GRNT31200036, 20PRE35210043, and 20PRE35210392.

#### DISCLOSURES

No conflicts of interest, financial or otherwise, are declared by the authors.

#### AUTHOR CONTRIBUTIONS

S.W., R.J.R., and F.F. conceived and designed research; S.W., H.Z., Y.L., L.L., Y.G., F.J., X.F., J.R.J., M.L., W.G., E.G.-F., R.O.M., and F.F. performed experiments; S.W., Y.L., L.L., Y.G., F.J., R.J.R., and F.F. analyzed data; S.W., B.T.A., R.J.R., and F.F. interpreted results of experiments; S.W., Y.L., L.L., R.J.R., and F.F. prepared figures; S.W., R.J.R., and F.F. drafted manuscript; S.W., E.G.-F., R.O.M., M.R.P., R.L., B.T.A., R.J.R., and F.F. edited and revised manuscript; S.W., H.Z., Y.L., L.L., Y.G., F.J., X.F., J.R.J., M.L., W.G., E.G.-F., R.O.M., M.R.P., R.L., B.T.A., R.J.R., and F.F. approved final version of manuscript.

#### REFERENCES

- Ahnstedt H, Cao L, Krause DN, Warfvinge K, Säveland H, Nilsson OG, Edvinsson L. Male-female differences in upregulation of vasoconstrictor responses in human cerebral arteries. *PLoS One* 8: e62698, 2013. doi:10.1371/journal.pone.0062698.
- Attwell D, Buchan AM, Charpak S, Lauritzen M, Macvicar BA, Newman EA. Glial and neuronal control of brain blood flow. *Nature* 468: 232–243, 2010. doi:10.1038/nature09613.
- Baumbach GL, Heistad DD. Cerebral circulation in chronic arterial hypertension. *Hypertension* 12: 89–95, 1988. doi:10.1161/01.HYP.12.2.89.
- Baumbach GL, Heistad DD, Siems JE. Effect of sympathetic nerves on composition and distensibility of cerebral arterioles in rats. *J Physiol* 416: 123–140, 1989. doi:10.1113/jphysiol.1989.sp017753.
- Blomfield J, Farrar JF. The fluorescent properties of maturing arterial elastin. *Cardiovasc Res* 3: 161–170, 1969. doi:10.1093/cvr/3.2.161.
- Boumazza S, Arribas SM, Osborne-Pellegrin M, McGrath JC, Laurent S, Lacolley P, Challande P. Fenestrations of the carotid internal elastic lamina and structural adaptation in stroke-prone spontaneously hypertensive rats. *Hypertension* 37: 1101–1107, 2001. doi:10.1161/01.HYP.37.4.1101.
- Brayden JE, Halpern W, Brann LR. Biochemical and mechanical properties of resistance arteries from normotensive and hypertensive rats. *Hypertension* 5: 17–25, 1983. doi:10.1161/01.HYP.5.1.17.
- Brayden JE, Nelson MT. Regulation of arterial tone by activation of calcium-dependent potassium channels. *Science* 256: 532–535, 1992. doi:10.1126/science.1373909.
- Briones AM, González JM, Somoza B, Giraldo J, Daly CJ, Vila E, González MC, McGrath JC, Arribas SM. Role of elastin in spontaneously hypertensive rat small mesenteric artery remodeling. *J Physiol* 552: 185–195, 2003. doi:10.1113/jphysiol.2003.046904.
- Chai Q, Wang XL, Zeldin DC, Lee HC. Role of caveolae in shear stress-mediated endothelium-dependent dilation in coronary arteries. *Cardiovasc Res* 100: 151–159, 2013. doi:10.1093/cvr/cvt157.
- Chan SL, Chapman AC, Sweet JG, Gokina NI, Cipolla MJ. Effect of PPAR $\gamma$  inhibition during pregnancy on posterior cerebral artery function and structure. *Front Physiol* 1: 130, 2010. doi:10.3389/fphys.2010.00130.
- Cheng JH, Zhang LF, Gao F, Bai YG, Boscolo M, Huang XF, Zhang X. Mechanics and composition of middle cerebral arteries from simulated microgravity rats with and without 1-h/d -Gx gravitation. *PLoS One* 9: e97737, 2014. doi:10.1371/journal.pone.0097737.
- Csipo T, Lipecz A, Fulop GA, Hand RA, Ngo BN, Dzialendzik M, Tarantini S, Balasubramanian P, Kiss T, Yabluchanska V, Silva-Palacios F, Courtney DL, Dasari TW, Sorond F, Sonntag WE, Csiszar A, Ungvari Z, Yabluchanskiy A. Age-related decline in peripheral vascular health predicts cognitive impairment. *Geroscience* 41: 125–136, 2019. doi:10.1007/s11357-019-00063-5.
- Csipo T, Mukli P, Lipecz A, Tarantini S, Bahadli D, Abdulhussein O, Owens C, Kiss T, Balasubramanian P, Nyúl-Tóth Á, Hand RA, Yabluchanska V, Sorond FA, Csiszar A, Ungvari Z, Yabluchanskiy A. Assessment of age-related decline of neurovascular coupling responses by functional near-infrared spectroscopy (fNIRS) in humans. *Geroscience* 41: 495–509, 2019. doi:10.1007/s11357-019-00122-x.
- Csiszar A, Tarantini S, Fülöp GA, Kiss T, Valcarcel-Ares MN, Galvan V, Ungvari Z, Yabluchanskiy A. Hypertension impairs neurovascular coupling and promotes microvascular injury: role in exacerbation of Alzheimer's disease. *Geroscience* 39: 359–372, 2017. doi:10.1007/s11357-017-9991-9.
- Dagenais GR, Leong DP, Rangarajan S, Lanan F, Lopez-Jaramillo P, Gupta R, Diaz R, Avezum A, Oliveira GBF, Wielgosz A, Parumbath SR, Mony P, Alhabib KF, Temizhan A, Ismail N, Chifamba J, Yeates K, Khatib R, Rahman O, Zatonska K, Kazmi K, Wei L, Zhu J, Rosengren A, Vijayakumar K, Kaur M, Mohan V, Yusufali A, Keli-shadi R, Teo KK, Joseph P, Yusuf S. Variations in common diseases, hospital admissions, and deaths in middle-aged adults in 21 countries from five continents (PURE): a prospective cohort study. *Lancet* 395: 785–794, 2020. doi:10.1016/S0140-6736(19)32007-0.
- Dayton A, Exner EC, Bukowy JD, Stodola TJ, Kurth T, Skelton M, Greene AS, Cowley AW Jr. Breaking the cycle: estrous variation does not require increased sample size in the study of female rats. *Hypertension* 68: 1139–1144, 2016. doi:10.1161/HYPERTENSIONAHA.116.08207.
- de Montgolfier O, Pouliot P, Gillis MA, Ferland G, Lesage F, Thorin-Trecases N, Thorin É. Systolic hypertension-induced neurovascular unit disruption magnifies vascular cognitive impairment in middle-age atherosclerotic LDLr<sup>-/-</sup>:hApoB<sup>+/+</sup> mice. *Geroscience* 41: 511–532, 2019. doi:10.1007/s11357-019-00070-6.
- Deegan BM, Sorond FA, Lipsitz LA, O'Leary G, Serrador JM. Gender related differences in cerebral autoregulation in older healthy subjects. *Conf Proc IEEE Eng Med Biol Soc* 2009: 2859–2862, 2009. doi:10.1109/IEMBS.2009.5333604.
- Dobrin PB. Mechanical properties of arteries. *Physiol Rev* 58: 397–460, 1978. doi:10.1152/physrev.1978.58.2.397.
- Euser AG, Cipolla MJ. Cerebral blood flow autoregulation and edema formation during pregnancy in anesthetized rats. *Hypertension* 49: 334–340, 2007. doi:10.1161/01.HYP.0000255791.54655.29.
- Fan F, Ge Y, Lv W, Elliott MR, Muroya Y, Hirata T, Booz GW, Roman RJ. Molecular mechanisms and cell signaling of 20-hydroxyeicosatetraenoic acid in vascular pathophysiology. *Front Biosci* 21: 1427–1463, 2016. doi:10.2741/4465.
- Fan F, Geurts AM, Murphy SR, Pabbidi MR, Jacob HJ, Roman RJ. Impaired myogenic response and autoregulation of cerebral blood flow is rescued in CYP4A1 transgenic Dahl salt-sensitive rat. *Am J Physiol Regul Integr Comp Physiol* 308: R379–R390, 2015. doi:10.1152/ajpregu.00256.2014.
- Fan F, Geurts AM, Pabbidi MR, Smith SV, Harder DR, Jacob H, Roman RJ. Zinc-finger nuclease knockout of dual-specificity protein phosphatase-5 enhances the myogenic response and autoregulation of cerebral blood flow in FHH.1BN rats. *PLoS One* 9: e112878, 2014. doi:10.1371/journal.pone.0112878.
- Fan F, Muroya Y, Roman RJ. Cytochrome P450 eicosanoids in hypertension and renal disease. *Curr Opin Nephrol Hypertens* 24: 37–46, 2015. doi:10.1097/MNH.000000000000088.
- Fan F, Pabbidi MR, Ge Y, Li L, Wang S, Mims PN, Roman RJ. Knockdown of Add3 impairs the myogenic response of renal afferent arterioles and middle cerebral arteries. *Am J Physiol Renal Physiol* 312: F971–F981, 2017. doi:10.1152/ajprenal.00529.2016.
- Fan F, Sun CW, Maier KG, Williams JM, Pabbidi MR, Didion SP, Falck JR, Zhuo J, Roman RJ. 20-Hydroxyeicosatetraenoic acid contributes to the inhibition of K<sup>+</sup> channel activity and vasoconstrictor response to angiotensin II in rat renal microvessels. *PLoS One* 8: e82482, 2013. doi:10.1371/journal.pone.0082482.
- Favre ME, Serrador JM. Sex differences in cerebral autoregulation are unaffected by menstrual cycle phase in young, healthy women. *Am J Physiol Heart Circ Physiol* 316: H920–H933, 2019. doi:10.1152/ajpheart.00474.2018.
- Fonck E, Feigl GG, Fasel J, Sage D, Unser M, Rüfenacht DA, Stergiopoulos N. Effect of aging on elastin functionality in human cerebral arteries. *Stroke* 40: 2552–2556, 2009. doi:10.1161/STROKEAHA.108.528091.

30. Gannon OJ, Robison LS, Custozzo AJ, Zuloaga KL. Sex differences in risk factors for vascular contributions to cognitive impairment & dementia. *Neurochem Int* 127: 38–55, 2019. doi:10.1016/j.neuint.2018.11.014.
31. Geary GG, Krause DN, Duckles SP. Estrogen reduces myogenic tone through a nitric oxide-dependent mechanism in rat cerebral arteries. *Am J Physiol* 275: H292–H300, 1998. doi:10.1152/ajpheart.1998.275.1.H292.
32. Gebremedhin D, Zhang DX, Weihrauch D, Uche NN, Harder DR. Detection of TRPV4 channel current-like activity in Fawn Hooded hypertensive (FHH) rat cerebral arterial muscle cells. *PLoS One* 12: e0176796, 2017. doi:10.1371/journal.pone.0176796.
33. Girijala RL, Sohrabji F, Bush RL. Sex differences in stroke: review of current knowledge and evidence. *Vasc Med* 22: 135–145, 2017. doi:10.1177/1358863X16668263.
34. González JM, Briones AM, Starcher B, Conde MV, Somoza B, Daly C, Vila E, McGrath I, González MC, Arribas SM. Influence of elastin on rat small artery mechanical properties. *Exp Physiol* 90: 463–468, 2005. doi:10.1113/expphysiol.2005.030056.
35. Gur RC, Gur RE, Obrist WD, Hungerbühler JP, Younkin D, Rosen AD, Skolnick BE, Reivich M. Sex and handedness differences in cerebral blood flow during rest and cognitive activity. *Science* 217: 659–661, 1982. doi:10.1126/science.7089587.
36. Hassler O. The windows of the internal elastic lamella of the cerebral arteries. *Virchows Arch Pathol Anat Physiol Klin Med* 335: 127–132, 1962. doi:10.1007/BF02438699.
37. Howe MD, Furr JW, Munshi Y, Roy-O'Reilly MA, Maniskas ME, Koellhoffer EC, d'Aigle J, Sansing LH, McCullough LD, Urayama A. Transforming growth factor- $\beta$  promotes basement membrane fibrosis, alters perivascular cerebrospinal fluid distribution, and worsens neurological recovery in the aged brain after stroke. *Geroscience* 41: 543–559, 2019. doi:10.1007/s11357-019-00118-7.
38. Hudetz AG. Incremental elastic modulus for orthotropic incompressible arteries. *J Biomech* 12: 651–655, 1979. doi:10.1016/0021-9290(79)90015-0.
39. Iadecola C, Davisson RL. Hypertension and cerebrovascular dysfunction. *Cell Metab* 7: 476–484, 2008. doi:10.1016/j.cmet.2008.03.010.
40. Izzard AS, Graham D, Burnham MP, Heerkens EH, Dominiczak AF, Heagerty AM. Myogenic and structural properties of cerebral arteries from the stroke-prone spontaneously hypertensive rat. *Am J Physiol Heart Circ Physiol* 285: H1489–H1494, 2003. doi:10.1152/ajpheart.00352.2003.
41. Karnik SK, Brooke BS, Bayes-Genis A, Sorensen L, Wythe JD, Schwartz RS, Keating MT, Li DY. A critical role for elastin signaling in vascular morphogenesis and disease. *Development* 130: 411–423, 2003. doi:10.1242/dev.00223.
42. Krejza J, Szydluk P, Liebeskind DS, Kochanowicz J, Bronov O, Mariak Z, Melhem ER. Age and sex variability and normal reference values for the V(MCA)/V(ICA) index. *AJNR Am J Neuroradiol* 26: 730–735, 2005.
43. Lamin V, Jaghoori A, Jakobczak R, Stafford I, Heresztyn T, Worthington M, Edwards J, Viana F, Stuklis R, Wilson DP, Beltrame JF. Mechanisms responsible for serotonin vascular reactivity sex differences in the internal mammary artery. *J Am Heart Assoc* 7: 007126, 2018. doi:10.1161/JAHA.117.007126.
44. Lee RM. Morphology of cerebral arteries. *Pharmacol Ther* 66: 149–173, 1995. doi:10.1016/0163-7258(94)00071-A.
45. Lindekleiv HM, Valen-Sendstad K, Morgan MK, Mardal KA, Faulder K, Magnus JH, Waterloo K, Romner B, Ingebrigtsen T. Sex differences in intracranial arterial bifurcations. *Genet Med* 7: 149–155, 2010. doi:10.1016/j.genm.2010.03.003.
46. Liu X, Li C, Falck JR, Roman RJ, Harder DR, Koehler RC. Interaction of nitric oxide, 20-HETE, and EETs during functional hyperemia in whisker barrel cortex. *Am J Physiol Heart Circ Physiol* 295: H619–H631, 2008. doi:10.1152/ajpheart.01211.2007.
47. Matteis M, Troisi E, Monaldi BC, Caltagirone C, Silvestrini M. Age and sex differences in cerebral hemodynamics: a transcranial Doppler study. *Stroke* 29: 963–967, 1998. doi:10.1161/01.STR.29.5.963.
48. McCarron JG, Osol G, Halpern W. Myogenic responses are independent of the endothelium in rat pressurized posterior cerebral arteries. *Blood Vessels* 26: 315–319, 1989.
49. McCarthy MM, Arnold AP, Ball GF, Blaustein JD, De Vries GJ. Sex differences in the brain: the not so inconvenient truth. *J Neurosci* 32: 2241–2247, 2012. doi:10.1523/JNEUROSCI.5372-11.2012.
50. Metz RP, Patterson JL, Wilson E. Vascular smooth muscle cells: isolation, culture, and characterization. *Methods Mol Biol* 843: 169–176, 2012. doi:10.1007/978-1-61779-523-7\_16.
51. Müller HR, Brunhölzl C, Radü EW, Buser M. Sex and side differences of cerebral arterial caliber. *Neuroradiology* 33: 212–216, 1991. doi:10.1007/BF00588220.
52. Navarro-Orozco D, Sanchez-Manso JC. *Neuroanatomy, Middle Cerebral Artery*. Treasure Island, FL: StatPearls Publishing, 2019.
53. Osol G, Osol R, Halpern W. Pre-existing level of tone is an important determinant of cerebral artery autoregulatory responsiveness. *J Hypertens Suppl* 7: S67–S69, 1989.
54. Pabbidi MR, Kuppusamy M, Didion SP, Sanapureddy P, Reed JT, Sontakke SP. Sex differences in the vascular function and related mechanisms: role of 17 $\beta$ -estradiol. *Am J Physiol Heart Circ Physiol* 315: H1499–H1518, 2018. doi:10.1152/ajpheart.00194.2018.
55. Pabbidi MR, Mazur O, Fan F, Farley JM, Gebremedhin D, Harder DR, Roman RJ. Enhanced large conductance K<sup>+</sup> channel activity contributes to the impaired myogenic response in the cerebral vasculature of Fawn Hooded Hypertensive rats. *Am J Physiol Heart Circ Physiol* 306: H989–H1000, 2014. doi:10.1152/ajpheart.00636.2013.
56. Peltonen GL, Harrell JW, Rousseau CL, Ernst BS, Marino ML, Crain MK, Schrage WG. Cerebrovascular regulation in men and women: stimulus-specific role of cyclooxygenase. *Physiol Rep* 3: e12451, 2015. doi:10.14814/phys2.12451.
57. Penley SC, Gaudet CM, Threlkeld SW. Use of an eight-arm radial water maze to assess working and reference memory following neonatal brain injury. *J Vis Exp* 4: 50940, 2013. doi:10.3791/50940.
58. Phillips AA, Matin N, Frias B, Zheng MM, Jia M, West C, Dorrance AM, Laher I, Krassioukov AV. Rigid and remodelled: cerebrovascular structure and function after experimental high-thoracic spinal cord transection. *J Physiol* 594: 1677–1688, 2016. doi:10.1113/JP270925.
59. Pires PW, Jackson WF, Dorrance AM. Regulation of myogenic tone and structure of parenchymal arterioles by hypertension and the mineralocorticoid receptor. *Am J Physiol Heart Circ Physiol* 309: H127–H136, 2015. doi:10.1152/ajpheart.00168.2015.
60. Pourageaud F, Crabos M, Freslon JL. The elastic modulus of conductance coronary arteries from spontaneously hypertensive rats is increased. *J Hypertens* 15: 1113–1121, 1997. doi:10.1097/00004872-199715100-00009.
61. Reed JT, Pareek T, Sriramula S, Pabbidi MR. Aging influences cerebrovascular myogenic reactivity and BK channel function in a sex-specific manner. *Cardiovasc Res* cvz314, 2019. doi:10.1093/cvr/cvz314.
62. Robison LS, Gannon OJ, Salinero AE, Zuloaga KL. Contributions of sex to cerebrovascular function and pathology. *Brain Res* 1710: 43–60, 2019. doi:10.1016/j.brainres.2018.12.030.
63. Sandow SL, Gzik DJ, Lee RM. Arterial internal elastic lamina holes: relationship to function? *J Anat* 214: 258–266, 2009. doi:10.1111/j.1469-7580.2008.01020.x.
64. Shatri J, Bexheti D, Bexheti S, Kabashi S, Krasniqi S, Ahmetgjakaj I, Zhjeqi V. Influence of gender and age on average dimensions of arteries forming the circle of willis study by magnetic resonance angiography on Kosovo's population. *Open Access Maced J Med Sci* 5: 714–719, 2017. doi:10.3889/oamjms.2017.160.
65. Shekhar S, Liu R, Travis OK, Roman RJ, Fan F. Cerebral autoregulation in hypertension and ischemic stroke: a mini review. *J Pharm Sci Exp Pharmacol* 2017: 21–27, 2017.
66. Shekhar S, Travis OK, He X, Roman RJ, Fan F. Menopause and ischemic stroke: A brief review. *MOJ Toxicol* 3: 00059, 2017.
67. Shekhar S, Varghese K, Li M, Fan L, Booz GW, Roman RJ, Fan F. Conflicting roles of 20-HETE in hypertension and stroke. *Int J Mol Sci* 20: 4500, 2019. doi:10.3390/ijms20184500.
68. Sherratt MJ. Tissue elasticity and the ageing elastic fibre. *Age (Dordr)* 31: 305–325, 2009. doi:10.1007/s11357-009-9103-6.
69. Simon JA, Hsia J, Cauley JA, Richards C, Harris F, Fong J, Barrett-Connor E, Hulley SB. Postmenopausal hormone therapy and risk of stroke: the heart and estrogen-progestin replacement study (HERS). *Circulation* 103: 638–642, 2001. doi:10.1161/01.CIR.103.5.638.
70. Smulyan H, Asmar RG, Rudnicki A, London GM, Safar ME. Comparative effects of aging in men and women on the properties of the arterial tree. *J Am Coll Cardiol* 37: 1374–1380, 2001. doi:10.1016/S0735-1097(01)01166-4.
71. Squair JW, Lee AH, Sarafis ZK, Chan F, Barak OF, Dujic Z, Day T, Phillips AA. Network analysis identifies consensus physiological mea-

- tures of neurovascular coupling in humans. *J Cereb Blood Flow Metab* 40: 656–666, 2020. doi:10.1177/0271678X19831825.
72. **Tarantini S, Tucsek Z, Valcarcel-Ares MN, Toth P, Gautam T, Giles CB, Ballabh P, Wei JY, Wren JD, Ashpole NM, Sonntag WE, Ungvari Z, Csiszar A.** Circulating IGF-1 deficiency exacerbates hypertension-induced microvascular rarefaction in the mouse hippocampus and retrosplenial cortex: implications for cerebrovascular and brain aging. *Age (Dordr)* 38: 273–289, 2016. doi:10.1007/s11357-016-9931-0.
  73. **Tarantini S, Yabluchanskiy A, Csipo T, Fulop G, Kiss T, Balasubramanian P, DelFavero J, Ahire C, Ungvari A, Nyúl-Tóth Á, Farkas E, Benyo Z, Tóth A, Csiszar A, Ungvari Z.** Treatment with the poly(ADP-ribose) polymerase inhibitor PJ-34 improves cerebrovascular endothelial function, neurovascular coupling responses and cognitive performance in aged mice, supporting the NAD<sup>+</sup> depletion hypothesis of neurovascular aging. *Geroscience* 41: 533–542, 2019. doi:10.1007/s11357-019-00101-2.
  74. **Toth P, Tarantini S, Csiszar A, Ungvari Z.** Functional vascular contributions to cognitive impairment and dementia: mechanisms and consequences of cerebral autoregulatory dysfunction, endothelial impairment, and neurovascular uncoupling in aging. *Am J Physiol Heart Circ Physiol* 312: H1–H20, 2017. doi:10.1152/ajpheart.00581.2016.
  75. **Toth P, Tarantini S, Springo Z, Tucsek Z, Gautam T, Giles CB, Wren JD, Koller A, Sonntag WE, Csiszar A, Ungvari Z.** Aging exacerbates hypertension-induced cerebral microhemorrhages in mice: role of resveratrol treatment in vasoprotection. *Aging Cell* 14: 400–408, 2015. doi:10.1111/accel.12315.
  76. **Toth P, Tucsek Z, Sosnowska D, Gautam T, Mitschelen M, Tarantini S, Deak F, Koller A, Sonntag WE, Csiszar A, Ungvari Z.** Age-related autoregulatory dysfunction and cerebrovascular injury in mice with angiotensin II-induced hypertension. *J Cereb Blood Flow Metab* 33: 1732–1742, 2013. doi:10.1038/jcbfm.2013.143.
  77. **Tryggestad JB, Thompson DM, Copeland KC, Short KR.** Sex differences in vascular compliance in normal-weight but not obese boys and girls: the effect of body composition. *Int J Pediatr* 2012: 1, 2012. doi:10.1155/2012/607895.
  78. **Ungvari Z, Tarantini S, Nyúl-Tóth Á, Kiss T, Yabluchanskiy A, Csipo T, Balasubramanian P, Lipecz A, Benyo Z, Csiszar A.** Nrf2 dysfunction and impaired cellular resilience to oxidative stressors in the aged vasculature: from increased cellular senescence to the pathogenesis of age-related vascular diseases. *Geroscience* 41: 727–738, 2019. doi:10.1007/s11357-019-00107-w.
  79. **Viscoli CM, Brass LM, Kernan WN, Sarrel PM, Suissa S, Horwitz RI.** A clinical trial of estrogen-replacement therapy after ischemic stroke. *N Engl J Med* 345: 1243–1249, 2001. doi:10.1056/NEJMoa010534.
  80. **Wagenseil JE, Mecham RP.** Vascular extracellular matrix and arterial mechanics. *Physiol Rev* 89: 957–989, 2009. doi:10.1152/physrev.00041.2008.
  81. **Wallis SJ, Firth J, Dunn WR.** Pressure-induced myogenic responses in human isolated cerebral resistance arteries. *Stroke* 27: 2287–2291, 1996. doi:10.1161/01.STR.27.12.2287.
  82. **Wang S, Jiao F, Guo Y, Zhang H, He X, Maranon RO, Alexandra B, Pabbidi MR, Roman RJ, Fan F.** Excessive salt consumption increases susceptibility to cerebrovascular dysfunction and cognitive impairments in the elderly of both sexes. *FASEB J* 33: 511–517, 2019.
  83. **Warrington JP, Fan F, Murphy SR, Roman RJ, Drummond HA, Granger JP, Ryan MJ.** Placental ischemia in pregnant rats impairs cerebral blood flow autoregulation and increases blood-brain barrier permeability. *Physiol Rep* 2: e12134, 2014. doi:10.14814/phy2.12134.
  84. **Welsh DG, Morielli AD, Nelson MT, Brayden JE.** Transient receptor potential channels regulate myogenic tone of resistance arteries. *Circ Res* 90: 248–250, 2002. doi:10.1161/hh0302.105662.
  85. **Yang SH, Shetty RA, Liu R, Sumien N, Heinrich KR, Rutledge M, Thangthaeng N, Brun-Zinkernagel AM, Forster MJ.** Endovascular middle cerebral artery occlusion in rats as a model for studying vascular dementia. *Age (Dordr)* 28: 297–307, 2006. doi:10.1007/s11357-006-9026-4.
  86. **Zimmerman MA, Budish RA, Kashyap S, Lindsey SH.** GPER-novel membrane oestrogen receptor. *Clin Sci (Lond)* 130: 1005–1016, 2016. doi:10.1042/CS20160114.